Lawrence Berkeley National Laboratory

Title

Large-Molecule Decomposition Products of Electrolytes and Additives Revealed by On-Electrode Chromatography and MALDI

Permalink

https://escholarship.org/uc/item/78b0n5zj

Journal

Joule, 5(2)

Authors

Fang, Chen
Lau, Jonathan
Hubble, Dion
et al.

Publication Date

2021-02-01

Peer reviewed

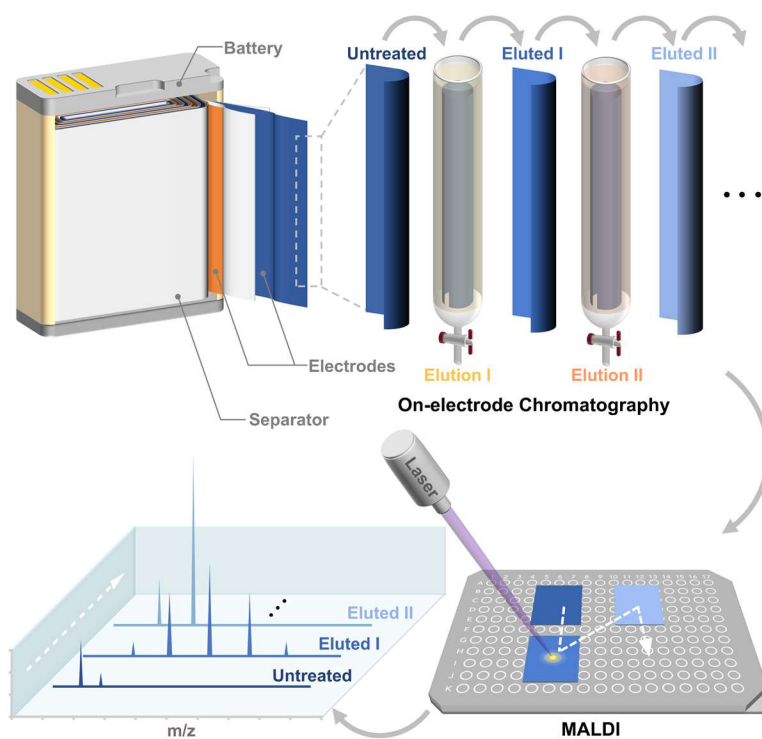**Large molecule decomposition products of electrolytes and additives revealed by on-electrode chromatography and MALDI**

Chen Fang[1], Jonathan Lau[1], Dion Hubble[1], Piyachai Khomein[1], Eric A. Dailing[2], Yi Liu[2,*] and Gao Liu[1,3,*]

[1]Energy Storage and Distributed Resources Division, Lawrence Berkeley National Laboratory, Berkeley, CA 94720, USA.

[2]The Molecular Foundry, Lawrence Berkeley National Laboratory, Berkeley, CA 94720, USA.

[3]Lead Contact.

* Correspondence: yliu@lbl.gov (Y.L.), gliu@lbl.gov (G.L.)

The decomposition of electrolyte and additive molecules has a critical impact on battery performance. In this work, large-molecule decomposition products in solid-electrolyte interphase (SEI) are identified with clear structure assignment by matrix-assisted laser desorption/ionization time-of-flight mass spectrometry (MALDI-TOF-MS). The MALDI analysis is facilitated by on-electrode chromatography that serves to fractionate different molecular species on the electrode surfaces prior to MS measurements. These methods exemplify a practical and readily adoptable strategy to characterize the organic elements in SEIs.

Lead Contact: gliu@lbl.gov

Summary

The solid-electrolyte interphase (SEI) produced by the decomposition of electrolyte has critical impact on battery performance. However, the precise makeup of SEI including the composition of organic and polymeric species, is one of the least understood aspects of lithium-ion batteries. Here, we probe the SEIs using Matrix-Assisted Laser Desorption/Ionization-Time of Flight mass spectrometry (MALDI-TOF-MS) assisted by on-electrode chromatography. On-electrode chromatography utilizes the electrode itself as the stationary phase for fractionating the molecules on the electrode surfaces, thus realizing separation of different molecular species prior to MALDI analysis. This strategy has proven important for effective MALDI measurements of SEI components directly on the electrode surfaces. With on-electrode chromatography, large molecule decomposition products of carbonate electrolytes containing vinylene carbonate and methacrylate additives are unambiguously illustrated in each case with clear structure assignment. This work provides a simple, powerful and universal solution for identification of the organic components in SEIs.

Keywords

Solid-electrolyte Interphase, MALDI, On-electrode Chromatography, Lithium-ion Battery, Electrolyte, Additive.
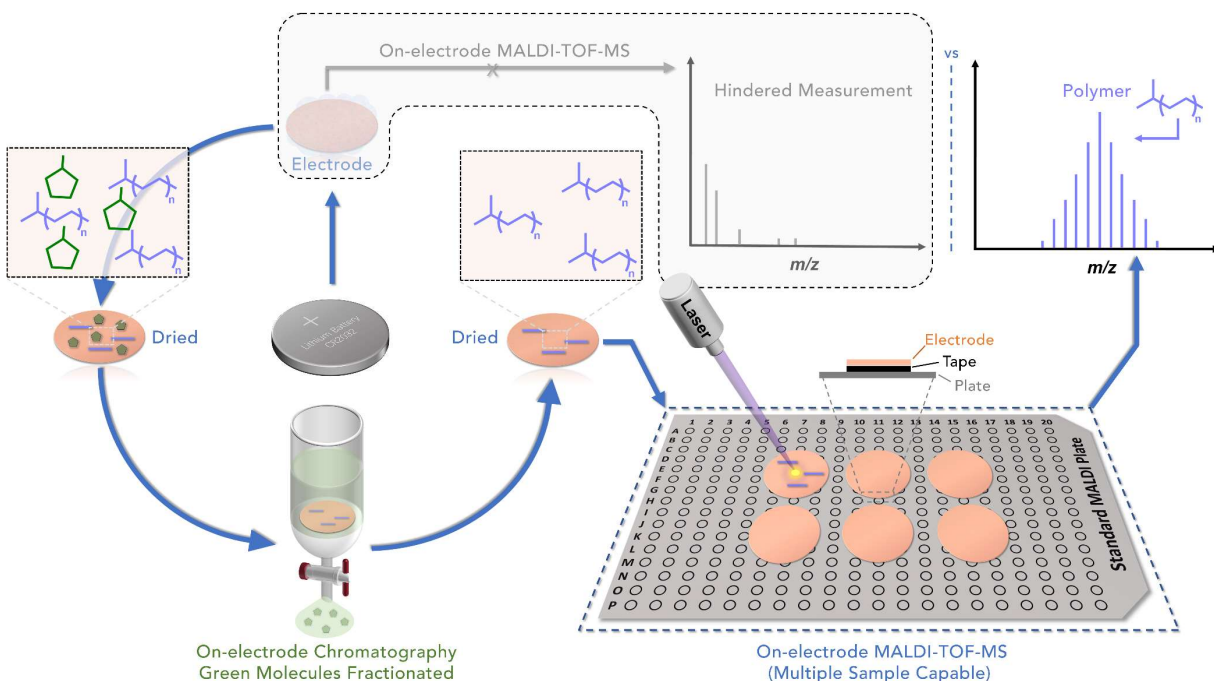
Introduction

Rechargeable batteries are crucial for contemporary society and play essential roles in electric vehicles (EVs), portable digital devices, large-scale electricity storage, etc.[1-6] Nevertheless, rechargeable batteries with increased cycle lifetime, energy density and cost efficiency are needed to power the coming clean energy revolution.[7,8] Consequently, the development of next-generation lithium-ion batteries (LIBs) has attracted tremendous research interest.[8-10] The challenges at the center of high energy and longer lifetime battery system are the reactivity of the electrolyte/electrode interface at potentials beyond the thermodynamic stability window of the electrolyte as well as the morphology change of the electrode surfaces during charge and discharge processes. Common electrolyte liquids for LIBs include carbonate solvents,[8,11] and the decomposition of these molecules leads to the formation of solid-electrolyte interphase (SEI) that dictates further interactions between the electrode and the bulk electrolyte.[11] In addition, additives have been incorporated into the electrolyte as sacrificial components to improve the SEI properties.[11,12] The decomposition reactions of electrolyte and additive molecules have been a key research focus for LIBs but the precise identification of the organic decomposition products has proven elusive.[13-16]

Many techniques have been employed for retrieving the elemental and bonding information of the SEI components, including X-ray photoelectron spectroscopy (XPS)[17-19], Fourier transform infrared spectroscopy (FTIR)[13,16,17,20], nuclear magnetic resonance (NMR)[14,15,21,22], etc. Mass spectrometry (MS) can identify the molecular and fragmental weights of the analytes and can hence provide critical information for clear assignment of the structures of the analytes. Gas chromatography mass spectrometry[23-25] (GC-MS) and liquid chromatography mass spectrometry [26,27] (LC-MS) can analyze volatile/gaseous and non-volatile electrolyte decomposition products, respectively. Nevertheless, GC/LC-MS methods require external chromatography for separation of the SEI components, which may not be chemically compatible

3

without removal of the destructive components.[28,29] To directly analyze the SEIs on electrode surfaces, secondary ion mass spectrometry (SIMS) has been developed as a depth-resolving MS tool, which makes SIMS an important and promising technique for SEI analysis.[30,31] SIMS ionizes SEI and electrolyte components with the primary ion beam, which generates small secondary ions and fragments that can reflect the dynamics of SEI formation. Due to the working mechanism of SIMS, it would experience difficulties in detecting large and fragile molecules in SEIs. Matrix-Assisted Laser Desorption/Ionization-Time of Flight mass spectrometry (MALDI-TOF-MS) is a MS method that can be employed for direct characterization of the electrode surfaces to identify organic and polymeric molecules in SEIs.[32-35] MALDI is a well-established MS technique that functions similarly to SIMS, differing in ionizing analytes by laser shots possibly with the assistance of matrix molecules for absorbing the laser energy.[36] The working principle of MALDI helps to reduce fragmentation and thus detect organic and polymer species in their molecular ion form, which provides key information for assignment of the exact structures of the molecular SEI elements. This is an important advantage of the MALDI technique. It has been demonstrated that MALDI has high sensitivity to track the chemical reaction of single layer of molecules on surfaces,[37,38] and therefore, MALDI is suitable for characterizing the small/trace amount of materials in SEIs. Nevertheless, the existing reports of MALDI studies of electrode samples suffer from low resolution of the spectra, bringing difficulties for spectrum analysis and assignment of electrolyte decomposition products.[34,35]

In this work, we couple MALDI with on-electrode chromatography to facilitate MALDI characterization of SEI components directly on the electrode (see Figure 1). Instead of solvent extraction of SEIs for external chromatography in GC/LC-MS measurements, on-electrode chromatography is employed to utilize the electrode surface as the stationary phase to realize controlled separation of the molecules on the electrode surfaces, which can be conveniently monitored with FTIR. With proper on-electrode

chromatography protocol, the SEI components of interest can be selectively retained and then measured by MALDI directly on the electrode surfaces. This approach bypasses the compatibility problem of external chromatography in GC/LC-MS moethods. The feasibility of on-electrode chromatography has been demonstrated with both Cu and silicon electrodes in our previous report.[39] In the present study, on-electrode chromatography prior to MALDI measurements has proven critical for effective MALDI analysis of SEIs. Decomposition reactions of carbonate electrolytes containing vinylene carbonate (VC) and triethylene glycol methyl ether methacrylate (TEGMA) additives are investigated individually, and high-mass polymeric decomposition products in SEIs have been unambiguously identified in each case with clear structure assignment.

Figure 1. Schematic depiction of electrode surface characterization by MALDI, assisted by on-electrode chromatography.
MALDI measurement of electrodes could be easily hindered by the complicated chemical environment on the electrode surfaces. Through proper solvent elution (left part of the figure) to fractionate different molecular species on electrode surfaces (such as ethylene carbonate, the green molecules), on-electrode chromatography can realize separation of the organic SEI components. This approach facilitates the MALDI detection of the organic electrolyte decomposition products in SEIs (right part of the figure), especially the high-mass polymeric species (the blue molecules). Multiple elution conditions

could be employed to separate and to distinguish different SEI components. The MALDI measurement is carried out with conventional MALDI instrumentation.

Results and Discussion

Decomposition of EC-based electrolyte and DHB matrix property

In this section, copper (Cu) electrodes cycled with 1.2M LiPF$_6$ EC/EMC electrolyte (ethylene carbonate/ethyl methyl carbonate, 3/7 w/w) are analyzed with on-electrode chromatography, FTIR, and MALDI as model system to investigate the decomposition product of EC-based electrolyte and the behaviors of matrix molecules. Matrix molecules are employed in MALDI measurements to assist ionization of the analytes, and therefore, the interpretation of MALDI spectra requires an accurate understanding of matrix behaviors. DHB (2,5-dihydroxybenzoic acid) is a common MALDI matrix[36] that has been used in previous MALDI studies of SEIs,[32-35] and it is thus employed in the present study. As the molecular weight of DHB is 154 Da, the low mass regions are covered in MALDI measurements to fully illustrate the behaviors of DHB matrix.
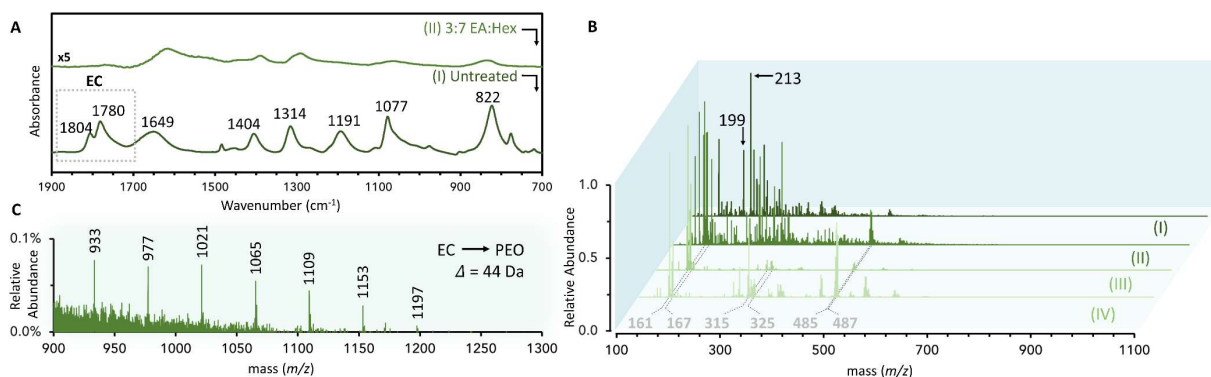
Figure 2. Characterization of Cu electrodes cycled with LiPF$_6$:EC/EMC electrolyte.
(A) FTIR spectra of electrodes (I) untreated and (II) treated with 3:7 EA:Hex elution. See also Figure S1.
(B) MALDI spectra of (BI) untreated electrode and electrodes treated with (BII) 3:7 EA:Hex elution, (BIII) EA elution and (BIV) DMC elution. (Black and grey color indicate signals originated from EC and DHB matrix, respectively.)
(C) Higher mass region of spectrum B-II demonstrating the presence of PEO species.

In our previous report,[39] we demonstrated that 3:7 ethyl acetate (EA):hexane (Hex) elution (v/v) could reliably remove residual EC electrolyte from the electrode surface, exposing underlying polymeric species. This controlled elution condition was the minimum polarity needed for separating EC, and would not lead to outstanding removal of the high-mass polymeric SEI components. Before carrying out MALDI analysis, the properness of 3:7 EA:Hex elution in the present study was examined by FTIR measurements. As shown in Figure 2A, the Cu electrode surface cycled with $LiPF_6$:EC/EMC electrolyte (Spectrum I) presented EC:$LiPF_6$ solvate[20,39] (1804, 1780, 1191, 1077, 822 cm^{-1}), $LiHCO_3$[39,40] (1649 cm^{-1}), and lithium ethylene di-carbonate[13,39] (LEDC, 1404, 1314 cm^{-1}), while on-electrode chromatography of 3:7 EA:Hex elution removed residual EC from the electrode surface (Spectrum II, as evidenced by the disappearance of EC's characteristic FTIR signals highlighted in Spectrum I). This result is consistent with our previous report. A more comprehensive analysis of Spectrum I is provided with Figure S1A. As this study focuses on the high-mass species in SEIs, the precise identity and behavior of LEDC are not pursued (alternative assignment could be lithium ethylene mono-carbonate, or LEMC).[13]

Stronger elution conditions with more polar solvents EA and dimethyl carbonate (DMC) were attempted in parallel tests. There was no outstanding FTIR signal observed on the electrode surfaces in these cases, indicating removal of the organic species (see Figure S1A). To further verify the properness of 3:7 EA:Hex elution, Nuclear Magnetic Resonance (NMR) study of the elution solution content was carried out, and there was no outstanding evidence that organic SEI species were present in the elution solution (see Figure S2 and Extended Discussion). Therefore, 3:7 EA:Hex elution was considered appropriate and was adopted to assist MALDI analysis. It is worth noting here that on-electrode chromatography is a general technique, and that elution conditions other than 3:7 EA:Hex could possibly be demanded for different interfaces, which can be systematically examined by gradient polarity solvent wash (gradient wash)

technique[39] to identify the optimum elution condition. FTIR can serve as a convenient complementary analytical tool to verify the properness of different elution conditions.

Next, MALDI measurements were carried out for the untreated and eluted Cu electrodes as shown in Figure 2B. The major peaks associated with DHB (grey) and EC (black) have been marked (assignments in Table 1). The behaviors of DHB matrix is firstly discussed here since the correct understanding of matrix properties is critical for MALDI data interpretation. DHB matrix is well-known to form clusters and be ionized by cations within the samples, possibly with mixed cations.[41-44] For example, $[DHB+Li]^+$ at 161 Da and $[3DHB-3H+4Li]^+$ at 487 Da are observed in Figure 2B, which were induced by the residual lithium salts that originated from the electrolyte. Lithiation of DHB clusters was observed together with Na^+ ion (Figure 2B, Table 1) presumably due to the ubiquitous presence of sodium element. Furthermore, DHB clusters could undergo fragmentation by losing water and carbonyl masses.[43-45] Therefore, the combined factors of DHB clustering, mixed cationization agents and fragmentation resulted in a series of matrix signals in MALDI measurements. Such mechanisms have been experimentally verified with DHB reference samples (see Figure S3 and Extended Discussion). The presence of DHB signals is a complication in DHB-based MALDI measurements. But on the other hand, these lithiated DHB species can be readily distinguished thanks to the lithium isotope effect. The lithium element occurs naturally as a mixture of ^6Li (7.52%) and ^7Li (92.48%) isotopes, which leads to an unique and relatively strong isotopic pattern at -1 Da position of the monoisotopic peaks.[46] Such an isotope effect is particularly pronounced for DHB clusters containing multiple lithium ions. Therefore, DHB-related signals can be identified easily by lithium isotope patterns.

With clarification of DHB matrix signals, the MALDI spectra were further analyzed to reveal the EC decomposition products. Without on-electrode chromatography elution, strong EC signals (Figure 2BI) were identified on the untreated electrode surface (higher mass region shown in Figure S1C). Upon 3:7

8

EA:Hex elution, EC was removed and no longer observed in MALDI measurement (Figure 2BII), which is consistent with FTIR results. The high-mass region of Figure 2BII is shown in Figure 2C, where a set of weak peaks separated by 44 Da was found between 900 and 1200 Da. Such a pattern could only be observed upon 3:7 EA:Hex elution, and it is attributed to polyethylene oxide (PEO), the decomposition product of EC-based electrolytes.[14,22,47] (The topic of PEO formation will be further developed in the next section.) It can be concluded that the residue electrolyte on the electrode surface hinders effective MALDI measurements of SEIs, and on-electrode chromatography is thus demanded for fractionating the organic species. In parallel tests, elution of the electrode samples with more polar solvents, namely EA and DMC, led to no outstanding MALDI signals other than DHB matrix (Figure 2BIII and 2BIV). These results confirmed the removal of organic species under polar elution conditions, which is in agreement with FTIR observations. Figure 2BIII and IV are further analyzed in the Supplementary Information (Figure S4A, Table S1) to demonstrate the possible DHB signals in MALDI measurement.
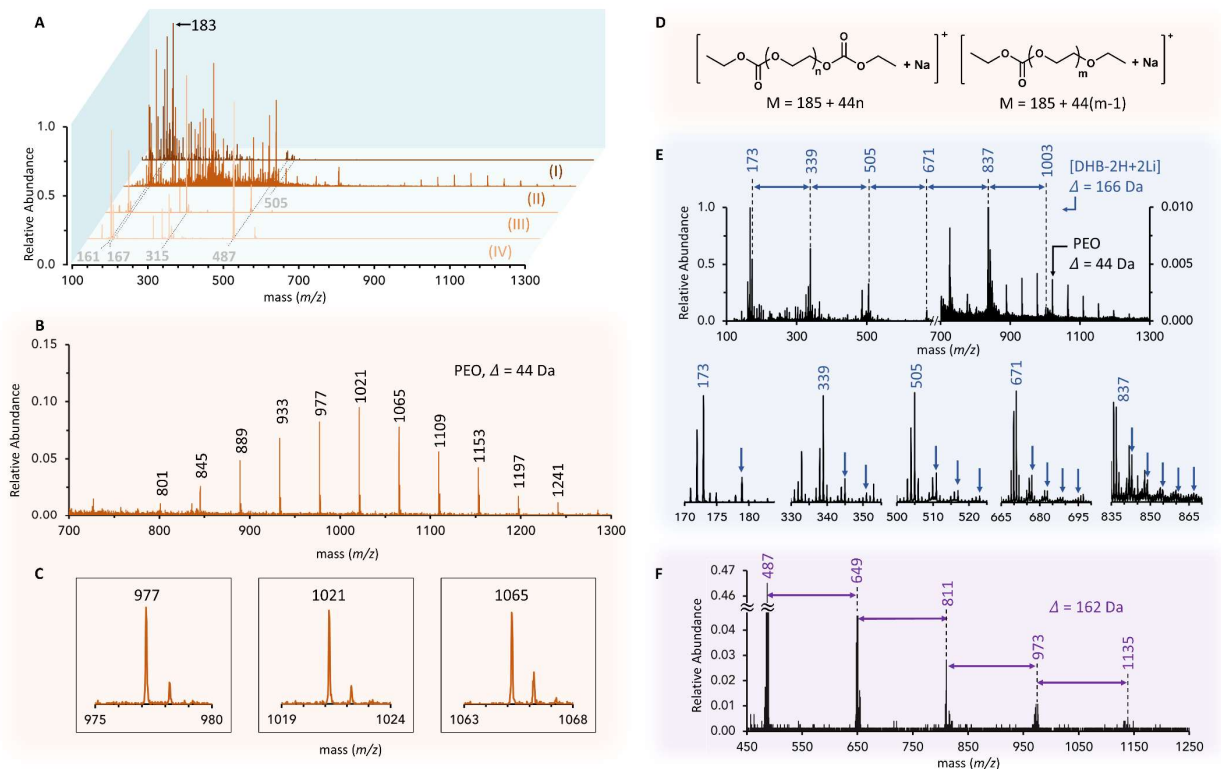
To briefly summarize, MALDI analysis assisted by on-electrode chromatography illustrated the formation of high-mass PEOs by decomposition of EC-based electrolyte, which could only be identified with proper on-electrode chromatography procedure. The on-electrode chromatography approach bypasses the complication of SEI extraction for external column-based chromatography and thus can serve as a convenient strategy to facilitate mass spectrometry analysis of SEIs by MALDI.
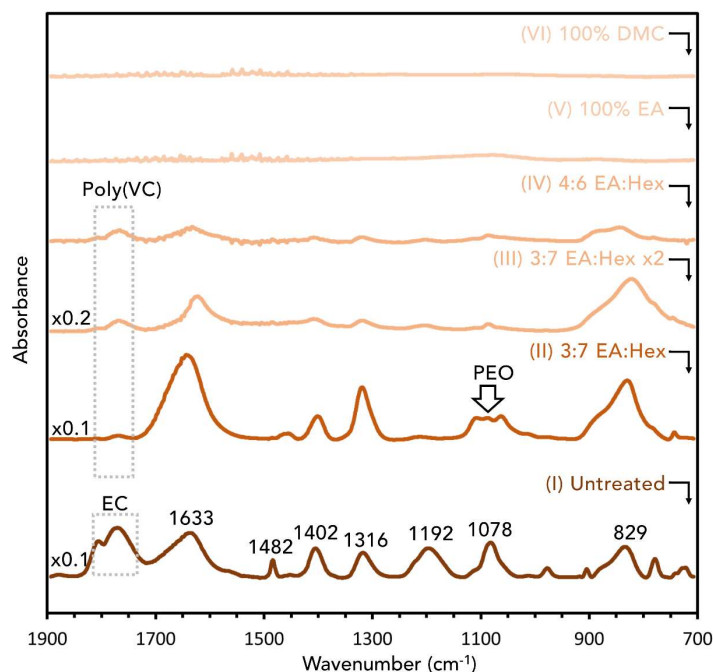
Figure 3. FTIR spectra of Cu electrodes cycled with LiPF$_6$:EC/EMC electrolyte containing VC additive.
(I) untreated electrode, and electrodes treated with (II) 3:7 EA:Hex elution, (III) 3:7 EA:Hex elution twice, (IV) 4:6 EA:Hex elution, (V) EA elution, and (VI) DMC elution. See also Figure S5.

Impact of vinylene carbonate on decomposition of EC-based electrolyte

Vinylene carbonate (VC) is one of the most commonly used additives for LIBs that can effectively improve the cell performance.[11] However, the precise electrochemical reaction pathway of VC is still under investigation.[16] It is known that decomposition of EC yields PEO,[14,22,47] and VC can affect the formation of PEO species.[15] PEO species can improve the ionic conductivity and increase the flexibility of the SEI.[48,49] Therefore, it is of interest to precisely identify the PEO species in SEIs. The impact of VC on the decomposition of EC-based electrolytes and formation of PEOs is explored in this section.

Figure 4. MALDI spectra of Cu electrodes cycled with LiPF$_6$:EC/EMC electrolyte containing VC additive.
(A) Electrodes after different elution treatments (I) untreated, (II) 3:7 EA:Hex elution, (III) EA elution and
(IV) DMC elution. (Black and grey color indicate signals originated from EC and DHB matrix, respectively.)
(B) High mass region of A-II expanded to demonstrate the PEO species.
(C) Isotope patterns of representative PEO signals.
(D) Possible PEO structures.
(E) 166 Da repeating pattern observed in MALDI measurement (top) and +6 Da patterns for each main
peak (bottom, marked by arrows). See also Figure S11.
(F) 162 Da repeating pattern observed in MALDI measurement. See also Figure S11.

Firstly, on-electrode chromatography procedure was examined for Cu electrodes cycled with VC additive

in LiPF$_6$:EC/EMC, as VC additive was not investigated in our previous study.[39] By FTIR measurement, it was

found that 3:7 EA:Hex elution remained effective for removal of residual EC electrolyte (Figure 3I vs 3II,

as evidenced by the disappearance of EC peaks). The full FTIR spectra of the samples in this section are

provided in Figure S5. After 3:7 EA:Hex elution, a broad peak around 1100 cm^{-1} (C-O-C stretching)

appeared (Figure 3II), which is attributed to the exposed PEO molecules.[50] This PEO signal was not clearly

observed for Cu electrode cycled without VC additive. In Figure 3II, there is another broad weak peak at

11

about 1770 cm^{-1} (carbonate C=O), and such a feature may indicate trace residual EC electrolyte that was not completely removed by elution. To verify the effectiveness of 3:7 EA:Hex elution procedure, stronger elution was conducted in parallel tests with either two rounds of 3:7 EA:Hex elution (Figure 3III) or a single round of 4:6 EA:Hex elution (Figure 3IV). The persistent presence of the 1770 cm^{-1} peak (highlighted in Figures 3II, III and IV) indicates that residual EC was unlikely the origin for this peak. Therefore, the 1770 cm^{-1} peak is attributed to poly(VC), which is structurally similar to EC and has been proposed as VC decomposition product.[21,51] Because the stronger elution conditions led to diminished PEO signal on FTIR spectra (also weak PEO signals in MALDI measurements, see Figure S6), 3:7 EA:Hex elution was adopted to avoid removal of organic species from the electrode surface. The post-elution 3:7 EA:Hex solution has been characterized by NMR, and there was no outstanding evidence that major organic SEI components were rinsed off (see Figure S2and Extended Discussion). Elution of parallel electrode samples by EA and DMC was also performed, and no outstanding FTIR signal was detected afterwards (Figures 3V and 3VI), indicating removal of organic species from the electrode.

With confirmation of on-electrode chromatography procedure, the MALDI analysis was carried out for Cu electrodes cycled with VC additive. As shown in Figure 4AI, the untreated electrode presented DHB (grey) and EC (black) (see Table 1). The higher mass region of Spectrum I is shown in Figure S1D. The 3:7 EA:Hex elution removed EC and allowed the detection of strong PEO signals in the 700-1300 Da range (Figure 4AII). The expanded PEO region is shown in Figure 4B. The strong PEO signals in both FTIR and MALDI measurements indicate that VC is possibly a promoter for the formation of PEOs around 1000 Da masses. No outstanding MALDI signals other than DHB matrix were detected for the electrode samples eluted with EA and DMC (Figures 4AIII and 4AIV, also see Figure S4B). These results agree with FTIR observations. As evidenced by FTIR, MALDI and NMR measurements, 3:7 EA:Hex elution would not result in destructive removal of the organic components in SEIs produced with VC additive. The isotope patterns of a few major

PEO signals in Figure 4B are shown in Figure 4C. There were +1 Da satellite peaks due to ^{13}C isotope but no -1 Da satellite peaks that would be characteristic of ^{6}Li isotope. Therefore, the PEOs were likely cationized by Na$^+$ ion instead of Li$^+$ ion (isotope patterns from Na$^+$ are negligible). The possible structures of PEO-sodium adducts are given in Figure 4D, which share the same series of masses and are consistent with previous reports.[23,24] It is worth noting here that previous MS studies demonstrated low-mass PEO species as decomposition products of EC-based electrolytes[22,47], while the present study illustrates the generation of high-mass PEO molecules (above 1000 Da) on electrode surfaces. The capability of MALDI in detection of high-mass molecules in their molecular ion form is a key advantage of MALDI technique as the precise molecular weight information helps to clarify the exact structures of the analytes.

As described earlier, post-elution FTIR measurements identified poly(VC) on the electrode surfaces, which was not extensively observed in MALDI measurements (see Figure S7 and Extended Discussion). Optimization of MALDI protocols might be demanded to specifically target at poly(VC) species. It is worth noting here that complementary analytical techniques such as FTIR are important for retrieving comprehensive SEI information to guide MALDI protocol development. Separately, non-cycled electrodes with or without VC additive have been processed with 3:7 EA:Hex elution and measured by MALDI. No PEO species were identified on the non-cycled electrodes (Figure S8), which verified that the high-mass PEOs were generated with electrochemical processes. The performances of silicon (Si) nanoparticle composite electrodes cycled with and without VC additive in LiPF$_6$:EC/EMC electrolyte are shown in Figure S9. It was found that VC led to higher specific capacity and Columbic Efficiency (CE). A detailed description is provided in Extended Discussion of Figure S9.

In the search for PEO species during MALDI measurements, two other unexpected polymer-like repeating features were observed, with 166 Da and 162 Da separation patterns, respectively. Both patterns have

been observed with or without the PEOs, indicating that they were not artifacts. The representative spectra are presented in Figures 4E and 4F, and the origins of these two patterns are discussed below. It has been verified that the MALDI signals observed on the electrodes did not originate from the tape materials used for attaching the electrodes (see Figure S10 and Extended Discussion), although precautions should always be taken to minimize the risk of tape-related contamination (see Supplemental Experimental Procedures).

The 166 Da repeating pattern in Figure 4E (top) was found with a Cu electrode cycled with VC additive and eluted with 3:7 EA:Hex. Although such a pattern highly resembles polymers, a careful examination of the spectrum revealed a few key features that suggest otherwise. As shown by the expanded spectra (Figure 4E, bottom), the polymer-like peaks at 173, 339, 505, 671, and 837 Da were accompanied by strong -1 Da isotope patterns, indicating high content of lithium. Additional satellite peaks at +6n Da positions were observed (highlighted by vertical arrows). The number of +6n Da satellite peaks was found identical as the apparent 'polymerization degree': for example, the 'pentamer' peak at 837 Da was associated with five sets of +6n satellite peaks at +6, +12, +18, +24, +30 Da positions. The +6 Da pattern can be observed when a proton of the analyte molecule is substituted by a lithium ion. Therefore, each 'polymer unit' should contain a reactive proton (e.g. -OH), which is unlikely possible for commonly accepted electrolyte decomposition products.[14-16] Consequently, the 166 Da repeating patterns is attributed to $[(DHB-2H+2Li)_n+Li]^+$, namely aggregates of lithiated DHB molecule [DHB-2H+2Li] (166 Da). Since each [DHB-2H+2Li] unit could allow one more Li^+ substitution, +6n satellite peaks were observed for these DHB aggregates. This rationale is also consistent with the observation of high lithium content. The 166 Da repeating pattern has been observed without the presence of PEOs as well (Figure S11A). To quickly summarize, the 166 Da repeating pattern is identified as highly lithiated DHB clusters as evidenced by their unique lithium substitution and lithium isotope patterns.
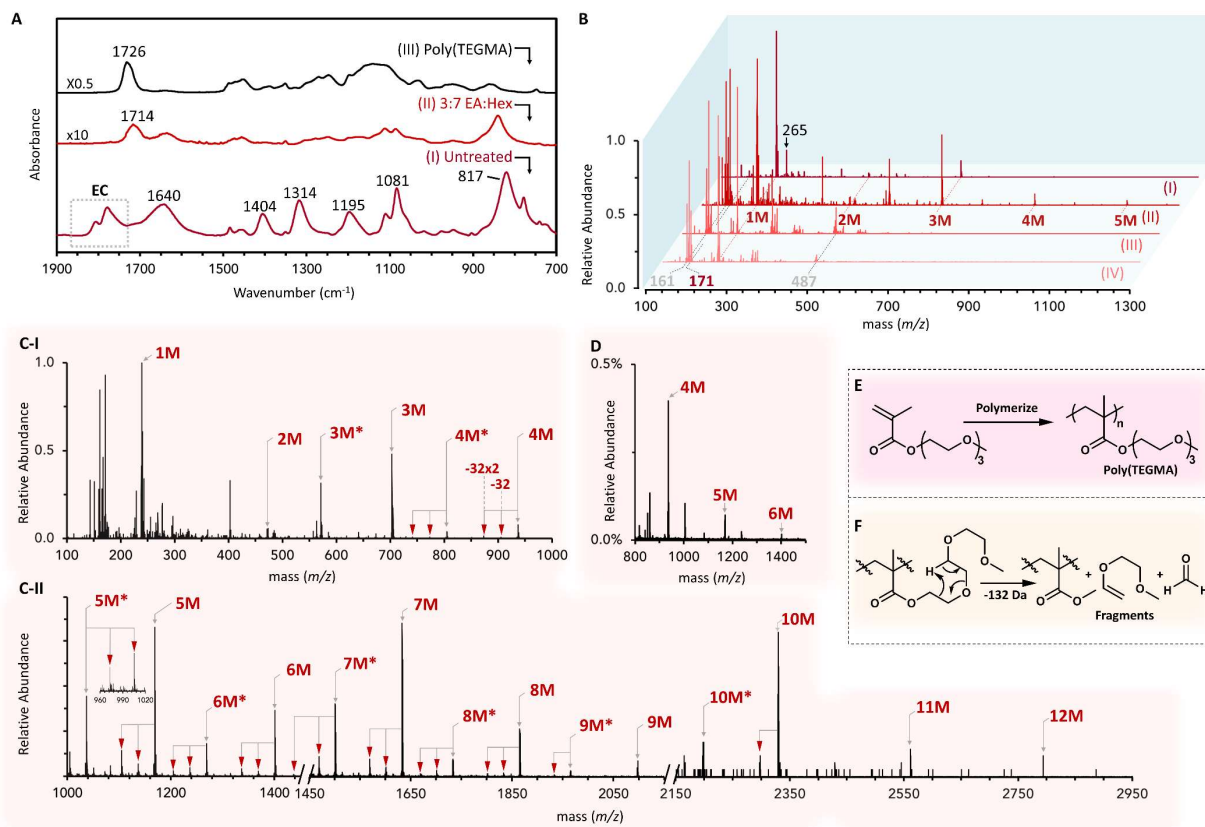
It should be stressed here that repeating mass patterns observed by MALDI must be carefully examined to conclude on their origination, since aggregates such as matrix clusters may generate 'fake' polymer patterns. It should also be emphasized that in-depth understanding of matrix properties is essential and critical for accurate MALDI analysis.

The 162 Da repeating pattern in Figure 4F was also observed for an electrode sample cycled with VC additive (eluted with 3:7 EA:Hex twice). Repeating patterns in similar mass ranges have been proposed to be polymeric electrolyte decomposition products.[32-34] The marked peaks are accompanied by +6 Da satellite peaks and strong -1 Da isotope peaks, indicating that these masses were likely partially composed of small lithium-DHB clusters. It is possible that the 162 Da repeating pattern originated from minor electrolyte decomposition products coupled with DHB/Li$^+$ aggregates, which is consistent with the observation that this pattern was only found above 400 Da. This 162 Da repeating pattern has been observed with PEOs as well (Figure S11B).

Polymerization of methacrylate additive

Methacrylate-based materials are widely investigated for applications in LIBs,[2,11] and the polymerization of methacrylates as sacrificial components in electrolyte is worth investigation. In our previous study,[39] polymerization of methacrylate additives was confirmed by FTIR but the polymer masses were not known. In the present study, the polymerization reaction of TEGMA additive (Figure 5E) is investigated by MALDI.

Figure 5. Characterization of Cu electrodes cycled with LiPF$_6$:EC/EMC electrolyte containing TEGMA additive. (1M through 12M in red color refer to TEGMA monomer through dodecamer.)

(A) FTIR spectra of (I) untreated electrode, (II) electrode treated with 3:7 EA:Hex elution, and (III) synthetic poly(TEGMA). See also Figure S1.

(B) MALDI spectra of (I) untreated electrode and electrodes treated with (II) 3:7 EA:Hex elution, (III) EA elution and (IV) DMC elution. (Black, grey and red colors indicate signals originated from EC, DHB and TEGMA, respectively.)

(C) (I) and (II) Full range MALDI spectrum of B-II demonstrating poly(TEGMA) species (asterisk mark indicates -132 Da fragmentation).

(D) High mass range of B-I.

(E) Polymerization of TEGMA additive.

(F) Fragmentation of triethylene glycol methyl ether chain of poly(TEGMA) molecules.

Firstly, FTIR measurements of the electrodes cycled with TEGMA after on-electrode chromatography treatments showed results consistent with the previous study. The untreated electrode surface (Figure 5A-I) was covered with residual EC electrolyte, which could be removed by 3:7 EA:Hex elution, exposing underlying poly(TEGMA) species (Figure 5AII) as confirmed with synthetic reference (Figure 5AIII). The

16

carbonyl group (1714 cm^{-1}) of poly(TEGMA) in Figure 5AII was found to experience a red shift due to solvation effect of lithium salt.[39] The 3:7 EA:Hex elution solution has been characterized by NMR and MALDI, and only TEGMA trimer was found in the elution solution (see Figure S2 and Extended Discussion). There was no outstanding evidence that high-mass TEGMA species were removed by 3:7 EA:Hex elution. In parallel tests, more extensive elution of the electrodes with EA and DMC resulted in removal of poly(TEGMA) species and exposure of lithium methacrylate on the electrode surface (Figure S1B), which originated from the decomposition of TEGMA.[39]

Next, the molecular weight of the poly(TEGMA) molecules was investigated by MALDI (Figure 5B-D, m/z values and assignments provided in Table S2). The untreated electrode surface presented EC (Figure 5BI, Table 1) and poly(TEGMA) species up to hexamer (Figure 5BI and 5D). The 171 Da peak is attributed to the lithium adduct of methyl triethylene glycol ether (TEGMA fragment). The higher mass region of the untreated electrode sample is shown in Figure S1E. Upon 3:7 EA:Hex elution, residual EC was removed and the TEGMA oligomers were identified by MALDI (Figure 5BII) with significantly higher signal intensities. The full spectrum is provided in Figures 5CI (<1000 Da) and 5CII (>1000 Da), illustrating up to TEGMA dodecamers. The structure assignment of poly(TEGMA) species are provided in Table S2, and the non-regular structures of TEGMA dimer and trimer[52] is explained in the Extended Discussion of Table S2. Two common fragmentation pathways of the poly(TEGMA) species have been identified. The pronounced fragmentation pattern involves the rearrangement of the triethylene glycol side chain of the poly(TEGMA) molecules presumably through a six-member-ring mechanism that leads to loss of 132 Da mass (Figure 5F).[53] The -132 Da fragments have been marked with asterisks in Figures 5C. Another minor fragmentation pathway involves the loss of the methanol mass (-32 Da) presumably by fragmentation of the terminal methoxy group of poly(TEGMA). Loss of one or two methanol masses have been observed for all the major poly(TEGMA) species (Figures 5C) as marked by red arrows linked to the corresponding parent peaks (see

Figure 5CI, the 4M peak as an example). These well-defined fragmentation pathways identified with high-quality spectra helped to endorse the assignment of poly(TEGMA) molecules.

The cycled electrode samples that were eluted with EA and DMC were also examined by MALDI. Poly(TEGMA) species were not found for these two samples (Figure 5BIII and 5BIV), and only DHB signals were observed (also see Figure S4C). Yet, TEGMA-Li$^+$ adduct (1M, 239 Da) was clearly observed in both cases, which is rationalized as the adsorption of the methacrylate molecules on the Cu electrode surface.[54] It is worth briefly noting here that the low-mass regions should be examined in MALDI measurements to constitute a comprehensive understanding of the SEI components. The FTIR and MALDI characterization of poly(TEGMA) species described above verified that 3:7 EA:Hex elution would not lead to significant removal of the large molecule components in SEIs, which was also supported by NMR studies of the elution solution (see Figure S2 and Extended Discussion).

The results in this section further demonstrated the benefit of on-electrode chromatography for MALDI analysis of electrode samples. There were three levels in fractionating the molecules on the electrode surfaces: (1) untreated electrode surface showed only low-mass TEGMA oligomers; (2) 3:7 EA:Hex elution removed residue electrolyte and led to detection of high-mass TEGMA oligomers; and (3) EA/DMC elution removed most of the organic species and revealed adsorbed TEGMA monomers on Cu electrode. The combined approaches of FTIR, on-electrode chromatography and MALDI fully illustrated the polymerization reactions of TEGMA additive, which could provide useful insights for tuning the electrochemical procedures for additive decomposition.

The universality of MALDI and on-electrode chromatography techniques has been demonstrated with SiO$_x$ and graphite electrodes cycled with TEGMA additive (Figure S12). For both types of electrodes, only

TEGMA trimer could be observed without on-electrode chromatography treatment while 3:7 EA:Hex elution revealed the presence of up to TEGMA hexamers. The performance of Si electrode cycled with TEGMA additive is shown in Figure S9, and TEGMA additive resulted in higher specific capacity and CE than the base electrolyte. The correlation of cell performance and SEI composition is presented in the Extended Discussion of Figure S9.

Conclusions

The on-electrode chromatography technique was employed to facilitate MALDI analysis of organic and polymeric species in SEIs by fractionating different components on the electrode surfaces. High-mass PEO and poly(TEGMA) molecules have been identified as electrolyte and additive decomposition products with clear structure assignment based on masses, isotope patterns, and fragmentation pathways. In addition, the DHB matrix was found capable of forming clusters upon lithiation to produce a range of signals including polymer-like repeating mass patterns, which highlights the necessity of careful examination of observed mass features in MALDI measurements. This work demonstrates that conventional MALDI technique in conjunction with on-electrode chromatography is a convenient and powerful method for identification of the exact molecular structures of organic and polymer components in SEIs. The universality of the introduced methods for SEI characterization has been demonstrated with Cu, SiO_x and graphite electrodes. As the only prerequisite for MALDI approach is the moderate electrical conductivity of the electrode sample, MALDI could be applied to various battery systems for characterization and rational design of the SEIs.

Experimental Procedures

Resource Availability

Lead Contact

Further information and requests for resources and materials should be directed to and will be fulfilled by the Lead Contact, Gao Liu (gliu@lbl.gov).

Materials Availability

This study did not generate new unique materials.

Data and Code Availability

This study did not generate code.

Materials

1.2 M LiPF$_6$ Ethylene Carbonate/Ethyl Methyl Carbonate (EC/EMC 3:7 w/w) electrolyte (Tomiyama Pure Chemical Industries, LTD), vinylene carbonate (VC, Sigma), triethylene glycol methyl ether methacrylate (TEGMA, Sigma) and 2,5-dihydroxybenzoic acid (DHB, Sigma) were used as received. The electrolyte has a water content of less than 20 ppm. Additive-containing electrolytes were made with 5wt% of the corresponding additive. Copper (Cu) electrodes 9/16" in diameter were punched from Cu foil. The synthetic poly(TEGMA) reference sample was obtained as previously reported.[39]

Procedures

The cell assembly and electrochemical protocols are adopted from our previous study[39] and are briefly described as follows. 2325 type coin cells (National Research Council, Canada) were assembled with Cu electrodes in a glovebox using Celgard 2400 separators (Celgard). The counter electrode was lithium metal electrode made from lithium foil (Albemarle), and the electrolyte used was 1.2 M LiPF$_6$ EC/EMC (3:7 w/w). In the cases where VC and TEGMA additives were applied, 5wt% of additives were incorporated. The electrochemical discharge of the assembled cell was carried out with linear sweep voltammetry on a

Maccor Series 4200 Battery Tester at 30°C from open-circuit voltage (OCV) to 50 mV vs Li/Li$^+$ at a sweep rate of 1 mV s^{-1}, followed by a potentiostatic hold at 50 mV for 2 hours. The linear sweep voltammetry allows precise control of the discharge process of Cu electrodes as the Cu model electrodes have no actual capacity. The potentiostatic hold step allows completion of the chemistry to generate SEIs comparable to those formed on actual battery electrodes. This adopted protocol also helps to ensure the comparability of the data to the previous report and between different samples. The cycled cells were opened under inert atmosphere to recover the Cu electrodes, which were immediately dried under vacuum to minimize further evolution of the SEI layers and were stored under inert atmosphere.

The on-electrode chromatography and FTIR procedures were adopted from the gradient polarity solvent wash technique in our previous report.[39] To briefly summarize, the Cu electrode was eluted with 5 ml solvents of choice in glass vials by manual agitation for 30 seconds. The electrode was then taken out from the solvent and immediately dried thoroughly under vacuum. Electrode samples eluted with different solvents were prepared in parallel. Both on-electrode chromatography and FTIR (Thermo Nicolet iS50, 32 scans at 4 cm^{-1} with reflective apparatus) were carried out as quickly as possible to minimize air exposure. The electrode samples were stored in air-isolated conditions and were transferred in sealed vials.

MALDI-TOF-MS measurements were performed on AB SCIEX TF4800 MALDI TOF-TOF Mass Spectrometer in reflector mode (positive mode, up to 4000 m/z) using DHB as matrix. It is worth briefly noting here that DHB is not the sole choice for MALDI matrix and other aprotic matrices are readily available (e.g. 9-nitroanthracene). The instrument was equipped with a Nd:YAG laser (355 nm wavelength, 3 to 7 ns pulse width, 200 Hz firing rate), and the spectra were collected in the 50-4000 Da range. The mass spectra were acquired from averaging of 400 laser shots. The matrix was applied to the electrode surface in tetrahydrofuran (THF) solution (10 mg/ml) before the electrode was fixed onto a standard 384-spot

MALDI sample plate with double-side conductive tape (Ted Pella, Inc). The THF solvent evaporated quickly due to its high volatility so that the matrix application could be performed fast under ambient condition. The use of double-side tape for sample attachment helps to conveniently and quickly complete the operation to minimize air exposure of the electrode samples. The MALDI plate was then immediately transferred into MALDI instrument (operating under vacuum).

Supplementary Information

Supplementary Information includes twelve figures and two tables and can be found with this article online at https://doi.org/10.1016.joule.XXXX.XX.XXX.

Author Contributions

C.F. and G.L. conceived the research. C.F. performed the experiments. P.K. prepared polymer materials. C.F. and E.D. established MALDI procedures. C.F., J.L. and D.H. established electrochemical procedures. C.F., D.H., P.K. and G.L. analyzed the data. C.F., J.L., D.H. and G.L. prepared the manuscript with input from all the other coauthors. Y.L. and G.L. supervised the research.

Declaration of Interests

The authors declare no competing interests.

References

1. Xu, R., Zhang, X.-Q., Cheng, X.-B., Peng, H.-J., Zhao, C.-Z., Yan, C., and Huang, J.-Q. (2018). Artificial Soft–Rigid Protective Layer for Dendrite-Free Lithium Metal Anode. Adv. Funct. Mater. *28*, 1705838.
2. Tan, S.-J., Zeng, X.-X., Ma, Q., Wu, X.-W., and Guo, Y.-G. (2018). Recent Advancements in Polymer-Based Composite Electrolytes for Rechargeable Lithium Batteries. Electrochem. Energy Rev. *1*, 113-138.
3. Lu, J., Chen, Z., Pan, F., Cui, Y., and Amine, K. (2018). High-Performance Anode Materials for Rechargeable Lithium-Ion Batteries. Electrochem. Energy Rev. *1*, 35-53.
4. Dunn, B., Kamath, H., and Tarascon, J.-M. (2011). Electrical Energy Storage for the Grid: A Battery of Choices. Science *334*, 928-935.
5. Fang, C., Zhang, G., Lau, J., and Liu, G. (2019). Recent advances in polysulfide mediation of lithium-sulfur batteries via facile cathode and electrolyte modification. APL Mater. *7*, 080902.
6. Li, Z., Fang, C., Qian, C., Zhou, S., Song, X., Ling, M., Liang, C., and Liu, G. (2019). Polyisoprene Captured Sulfur Nanocomposite Materials for High-Areal-Capacity Lithium Sulfur Battery. ACS Appl. Polym. Mater. *1*, 1965-1970.
7. Goodenough, J.B., and Park, K.-S. (2013). The Li-Ion Rechargeable Battery: A Perspective. J. Am. Chem. Soc. *135*, 1167-1176.
8. Xu, Z., Yang, J., Li, H., Nuli, Y., and Wang, J. (2019). Electrolytes for advanced lithium ion batteries using silicon-based anodes. J. Mater. Chem. A *7*, 9432-9446.
9. McDowell, M.T., Lee, S.W., Nix, W.D., and Cui, Y. (2013). 25th Anniversary Article: Understanding the Lithiation of Silicon and Other Alloying Anodes for Lithium-Ion Batteries. Adv. Mater. *25*, 4966-4985.
10. Zhou, S., Fang, C., Song, X., and Liu, G. (2020). The influence of compact and ordered carbon coating on solid-state behaviors of silicon during electrochemical processes. Carbon Energy *2*, 143-150.
11. Shin, J., Kim, T.-H., Lee, Y., and Cho, E. (2020). Key functional groups defining the formation of Si anode solid-electrolyte interphase towards high energy density Li-ion batteries. Energy Storage Mater. *25*, 764-781.
12. Haregewoin, A.M., Wotango, A.S., and Hwang, B.-J. (2016). Electrolyte additives for lithium ion battery electrodes: progress and perspectives. Energy Environ. Sci. *9*, 1955-1988.
13. Wang, L., Menakath, A., Han, F., Wang, Y., Zavalij, P.Y., Gaskell, K.J., Borodin, O., Iuga, D., Brown, S.P., Wang, C.*, et al.* (2019). Identifying the components of the solid–electrolyte interphase in Li-ion batteries. Nat. Chem. *11*, 789-796.
14. Jin, Y., Kneusels, N.-J.H., Magusin, P.C.M.M., Kim, G., Castillo-Martínez, E., Marbella, L.E., Kerber, R.N., Howe, D.J., Paul, S., Liu, T.*, et al.* (2017). Identifying the Structural Basis for the Increased Stability of the Solid Electrolyte Interphase Formed on Silicon with the Additive Fluoroethylene Carbonate. J. Am. Chem. Soc. *139*, 14992-15004.
15. Jin, Y., Kneusels, N.-J.H., Marbella, L.E., Castillo-Martínez, E., Magusin, P.C.M.M., Weatherup, R.S., Jónsson, E., Liu, T., Paul, S., and Grey, C.P. (2018). Understanding Fluoroethylene Carbonate and Vinylene Carbonate Based Electrolytes for Si Anodes in Lithium Ion Batteries with NMR Spectroscopy. J. Am. Chem. Soc. *140*, 9854-9867.
16. Grugeon, S., Jankowski, P., Cailleu, D., Forestier, C., Sannier, L., Armand, M., Johansson, P., and Laruelle, S. (2019). Towards a better understanding of vinylene carbonate derived SEI-layers by synthesis of reduction compounds. J. Power Sources *427*, 77-84.

17. Nie, M., Abraham, D.P., Seo, D.M., Chen, Y., Bose, A., and Lucht, B.L. (2013). Role of Solution Structure in Solid Electrolyte Interphase Formation on Graphite with LiPF6 in Propylene Carbonate. J. Phys. Chem. C *117*, 25381-25389.

18. Lu, P., Li, C., Schneider, E.W., and Harris, S.J. (2014). Chemistry, Impedance, and Morphology Evolution in Solid Electrolyte Interphase Films during Formation in Lithium Ion Batteries. J. Phys. Chem. C *118*, 896-903.

19. Herstedt, M., Andersson, A.M., Rensmo, H., Siegbahn, H., and Edström, K. (2004). Characterisation of the SEI formed on natural graphite in PC-based electrolytes. Electrochim. Acta *49*, 4939-4947.

20. Zhuang, G.V., Xu, K., Yang, H., Jow, T.R., and Ross, P.N. (2005). Lithium Ethylene Dicarbonate Identified as the Primary Product of Chemical and Electrochemical Reduction of EC in 1.2 M LiPF6/EC:EMC Electrolyte. J. Phys. Chem. B *109*, 17567-17573.

21. Ota, H., Sakata, Y., Inoue, A., and Yamaguchi, S. (2004). Analysis of Vinylene Carbonate Derived SEI Layers on Graphite Anode. J. Electrochem. Soc. *151*, A1659.

22. Jin, Y., Kneusels, N.-J.H., and Grey, C.P. (2019). NMR Study of the Degradation Products of Ethylene Carbonate in Silicon–Lithium Ion Batteries. The Journal of Physical Chemistry Letters *10*, 6345-6350.

23. Sloop, S.E., Kerr, J.B., and Kinoshita, K. (2003). The role of Li-ion battery electrolyte reactivity in performance decline and self-discharge. J. Power Sources *119-121*, 330-337.

24. Gireaud, L., Grugeon, S., Pilard, S., Guenot, P., Tarascon, J.-M., and Laruelle, S. (2006). Mass Spectrometry Investigations on Electrolyte Degradation Products for the Development of Nanocomposite Electrodes in Lithium Ion Batteries. Anal. Chem. *78*, 3688-3698.

25. Campion, C.L., Li, W., and Lucht, B.L. (2005). Thermal Decomposition of LiPF[sub 6]-Based Electrolytes for Lithium-Ion Batteries. J. Electrochem. Soc. *152*, A2327.

26. Tochihara, M., Nara, H., Mukoyama, D., Yokoshima, T., Momma, T., and Osaka, T. (2015). Liquid Chromatography-Quadruple Time of Flight Mass Spectrometry Analysis of Products in Degraded Lithium-Ion Batteries. J. Electrochem. Soc. *162*, A2008-A2015.

27. Schultz, C., Vedder, S., Streipert, B., Winter, M., and Nowak, S. (2017). Quantitative investigation of the decomposition of organic lithium ion battery electrolytes with LC-MS/MS. RSC Adv. *7*, 27853-27862.

28. Sahore, R., Dogan, F., and Bloom, I.D. (2019). Identification of Electrolyte-Soluble Organic Cross-Talk Species in a Lithium-Ion Battery via a Two-Compartment Cell. Chemistry of Materials *31*, 2884-2891.

29. Petibon, R., Rotermund, L., Nelson, K.J., Gozdz, A.S., Xia, J., and Dahn, J.R. (2014). Study of Electrolyte Components in Li Ion Cells Using Liquid-Liquid Extraction and Gas Chromatography Coupled with Mass Spectrometry. J. Electrochem. Soc. *161*, A1167-A1172.

30. Zhu, Z., Zhou, Y., Yan, P., Vemuri, R.S., Xu, W., Zhao, R., Wang, X., Thevuthasan, S., Baer, D.R., and Wang, C.-M. (2015). In Situ Mass Spectrometric Determination of Molecular Structural Evolution at the Solid Electrolyte Interphase in Lithium-Ion Batteries. Nano Lett. *15*, 6170-6176.

31. Zhou, Y., Su, M., Yu, X., Zhang, Y., Wang, J.-G., Ren, X., Cao, R., Xu, W., Baer, D.R., Du, Y.*, et al.* (2020). Real-time mass spectrometric characterization of the solid–electrolyte interphase of a lithium-ion battery. Nat. Nanotechnol. *15*, 224-230.

32. Tavassol, H., Buthker, J.W., Ferguson, G.A., Curtiss, L.A., and Gewirth, A.A. (2012). Solvent Oligomerization during SEI Formation on Model Systems for Li-Ion Battery Anodes. J. Electrochem. Soc. *159*, A730-A738.

33. Tavassol, H., Chan, M.K.Y., Catarello, M.G., Greeley, J., Cahill, D.G., and Gewirth, A.A. (2013). Surface Coverage and SEI Induced Electrochemical Surface Stress Changes during Li Deposition in a Model System for Li-Ion Battery Anodes. J. Electrochem. Soc. *160*, A888-A896.

34. Huff, L.A., Tavassol, H., Esbenshade, J.L., Xing, W., Chiang, Y.-M., and Gewirth, A.A. (2016). Identification of Li-Ion Battery SEI Compounds through 7Li and 13C Solid-State MAS NMR Spectroscopy and MALDI-TOF Mass Spectrometry. ACS Appl. Mater. Interfaces *8*, 371-380.

35. Abouimrane, A., Odom, S.A., Tavassol, H., Schulmerich, M.V., Wu, H., Bhargava, R., Gewirth, A.A., Moore, J.S., and Amine, K. (2012). 3-Hexylthiophene as a Stabilizing Additive for High Voltage Cathodes in Lithium-Ion Batteries. J. Electrochem. Soc. *160*, A268-A271.

36. Karas, M., and Krüger, R. (2003). Ion Formation in MALDI: The Cluster Ionization Mechanism. Chem. Rev. *103*, 427-440.

37. He, J., Fang, C., Shelp, R.A., and Zimmt, M.B. (2017). Tracking Invisible Transformations of Physisorbed Monolayers: LDI-TOF and MALDI-TOF Mass Spectrometry as Complements to STM Imaging. Langmuir *33*, 459-467.

38. Fang, C., Zhu, H., Chen, O., and Zimmt, M.B. (2018). Reactive two-component monolayers template bottom-up assembly of nanoparticle arrays on HOPG. Chem. Commun. *54*, 8056-8059.

39. Fang, C., Liu, Z., Lau, J., Elzouka, M., Zhang, G., Khomein, P., Lubner, S., Ross, P.N., and Liu, G. (2020). Gradient Polarity Solvent Wash for Separation and Analysis of Electrolyte Decomposition Products on Electrode Surfaces. J. Electrochem. Soc. *167*, 020506.

40. Zhuang, G.V., and Ross, P.N. (2003). Analysis of the Chemical Composition of the Passive Film on Li-Ion Battery Anodes Using Attenuated Total Reflection Infrared Spectroscopy. Electrochem. Solid-State Lett. *6*, A136.

41. Dannenberger, D., Süß, R., Teuber, K., Fuchs, B., Nuernberg, K., and Schiller, J. (2010). The intact muscle lipid composition of bulls: an investigation by MALDI-TOF MS and 31P NMR. Chem. Phys. Lipids *163*, 157-164.

42. Veličković, D., Herdier, H., Philippe, G., Marion, D., Rogniaux, H., and Bakan, B. (2014). Matrix-assisted laser desorption/ionization mass spectrometry imaging: a powerful tool for probing the molecular topology of plant cutin polymer. PLANT J *80*, 926-935.

43. Nimptsch, A., Schibur, S., Schnabelrauch, M., Fuchs, B., Huster, D., and Schiller, J. (2009). Characterization of the quantitative relationship between signal-to-noise (S/N) ratio and sample amount on-target by MALDI-TOF MS: Determination of chondroitin sulfate subsequent to enzymatic digestion. Anal. Chim. Acta *635*, 175-182.

44. Schiller, J., Süß, R., Fuchs, B., Müller, M., Petković, M., Zschörnig, O., and Waschipky, H. (2007). The suitability of different DHB isomers as matrices for the MALDI-TOF MS analysis of phospholipids: which isomer for what purpose? Eur. Biophys. J. *36*, 517-527.

45. Teearu, A., Vahur, S., Haljasorg, U., Leito, I., Haljasorg, T., and Toom, L. (2014). 2,5-Dihydroxybenzoic acid solution in MALDI-MS: ageing and use for mass calibration. J. Mass Spectrom. *49*, 970-979.

46. Stringano, E., Cramer, R., Hayes, W., Smith, C., Gibson, T., and Mueller-Harvey, I. (2011). Deciphering the Complexity of Sainfoin (Onobrychis viciifolia) Proanthocyanidins by MALDI-TOF Mass Spectrometry with a Judicious Choice of Isotope Patterns and Matrixes. Anal. Chem. *83*, 4147-4153.

47. Gachot, G., Grugeon, S., Armand, M., Pilard, S., Guenot, P., Tarascon, J.-M., and Laruelle, S. (2008). Deciphering the multi-step degradation mechanisms of carbonate-based electrolyte in Li batteries. J. Power Sources *178*, 409-421.

48. Zeng, W., Wang, L., Peng, X., Liu, T., Jiang, Y., Qin, F., Hu, L., Chu, P.K., Huo, K., and Zhou, Y. (2018). Enhanced Ion Conductivity in Conducting Polymer Binder for High-Performance Silicon Anodes in Advanced Lithium-Ion Batteries. Adv. Energy Mater. *8*, 1702314.

49. Assegie, A.A., Cheng, J.-H., Kuo, L.-M., Su, W.-N., and Hwang, B.-J. (2018). Polyethylene oxide film coating enhances lithium cycling efficiency of an anode-free lithium-metal battery. Nanoscale *10*, 6125-6138.

50. Wen, S.J., Richardson, T.J., Ghantous, D.I., Striebel, K.A., Ross, P.N., and Cairns, E.J. (1996). FTIR characterization of PEO + LiN(CF3SO2)2 electrolytes. J. Electroanal. Chem. *408*, 113-118.

51. Chai, J., Liu, Z., Ma, J., Wang, J., Liu, X., Liu, H., Zhang, J., Cui, G., and Chen, L. (2017). In Situ Generation of Poly (Vinylene Carbonate) Based Solid Electrolyte with Interfacial Stability for LiCoO2 Lithium Batteries. Adv. Sci *4*, 1600377.

52. Lingnau, J., Stickler, M., and Meyerhoff, G. (1980). The spontaneous polymerization of methyl methacrylate-IV: Formation of cyclic dimers and linear trimers. Eur. Polym. J. *16*, 785-791.

53. Marie, A., Fournier, F., and Tabet, J.C. (2000). Characterization of Synthetic Polymers by MALDI-TOF/MS: Investigation into New Methods of Sample Target Preparation and Consequence on Mass Spectrum Finger Print. Anal. Chem. *72*, 5106-5114.

54. Baute, N., Teyssié, P., Martinot, L., Mertens, M., Dubois, P., and Jérôme, R. (1998). Electrografting of Acrylic and Methacrylic Monomers onto Metals: Influence of the Relative Polarity and Donor–Acceptor Properties of the Monomer and the Solvent. Eur. J. Inorg. Chem. *1998*, 1711-1720.

Figures

Figure 1. Schematic depiction of electrode surface characterization by MALDI, assisted by on-electrode chromatography.
MALDI measurement of electrodes could be easily hindered by the complicated chemical environment on the electrode surfaces. Through proper solvent elution (left part of the figure) to fractionate different molecular species on electrode surfaces (such as ethylene carbonate, the green molecules), on-electrode chromatography can realize separation of the organic SEI components. This approach facilitates the MALDI detection of the organic electrolyte decomposition products in SEIs (right part of the figure), especially the high-mass polymeric species (the blue molecules). Multiple elution conditions could be employed to separate and to distinguish different SEI components. The MALDI measurement is carried out with conventional MALDI instrumentation.

Figure 2. Characterization of Cu electrodes cycled with LiPF$_6$:EC/EMC electrolyte.
(A) FTIR spectra of electrodes (I) untreated and (II) treated with 3:7 EA:Hex elution. See also Figure S1.
(B) MALDI spectra of (I) untreated electrode and electrodes treated with (II) 3:7 EA:Hex elution, (III) EA elution and (IV) DMC elution. (Black and grey color indicate signals originated from EC and DHB matrix, respectively.)
(C) Higher mass region of spectrum B-II demonstrating the presence of PEO species.

Figure 3. FTIR spectra of Cu electrodes cycled with LiPF$_6$:EC/EMC electrolyte containing VC additive.
(I) untreated electrode, and electrodes treated with (II) 3:7 EA:Hex elution, (III) 3:7 EA:Hex elution twice, (IV) 4:6 EA:Hex elution, (V) EA elution, and (VI) DMC elution. See also Figure S5.

Figure 4. MALDI spectra of Cu electrodes cycled with LiPF$_6$:EC/EMC electrolyte containing VC additive.
(A) Electrodes after different elution treatments (I) untreated, (II) 3:7 EA:Hex elution, (III) EA elution and (IV) DMC elution. (Black and grey color indicate signals originated from EC and DHB matrix, respectively.)
(B) High mass region of A-II expanded to demonstrate the PEO species.
(C) Isotope patterns of representative PEO signals.
(D) Possible PEO structures.
(E) 166 Da repeating pattern observed in MALDI measurement (top) and +6 Da patterns for each main peak (bottom, marked by arrows). See also Figure S11.
(F) 162 Da repeating pattern observed in MALDI measurement. See also Figure S11.

Figure 5. Characterization of Cu electrodes cycled with LiPF$_6$:EC/EMC electrolyte containing TEGMA additive. (1M through 12M in red color refer to TEGMA monomer through dodecamer.)
(A) FTIR spectra of (I) untreated electrode, (II) electrode treated with 3:7 EA:Hex elution, and (III) synthetic poly(TEGMA). See also Figure S1.
(B) MALDI spectra of (I) untreated electrode and electrodes treated with (II) 3:7 EA:Hex elution, (III) EA elution and (IV) DMC elution. (Black, grey and red colors indicate signals originated from EC, DHB and TEGMA, respectively.)
(C) (I) and (II) Full range MALDI spectrum of B-II demonstrating poly(TEGMA) species (asterisk mark indicates -132 Da fragmentation).
(D) High mass range of B-I.
(E) Polymerization of TEGMA additive.
(F) Fragmentation of triethylene glycol methyl ether chain of poly(TEGMA) molecules.

Table 1. Assignment of EC and DHB species in MALDI measurements.

m/z	Assignment	m/z	Assignment
161	DHB+Li	315	2DHB+Li
167	DHB-H+2Li	325	2DHB-H_2O-2H+2Li+Na
183	2EC+Li	485	3DHB-H_2O-3H+3Li+Na
199	2EC+Na	487	3DHB-3H+4Li
213	EC+DHB-2H_2O+Li	505	3DHB-6H+7Li
265	EC+DHB+Na		